Journal of Applied Physics

Long-time stable colloidal Zn–Ag–In–S quantum dots with tunable midgap-involved emission

Cite as: J. Appl. Phys. **129**, 063107 (2021); https://doi.org/10.1063/5.0038696
Submitted: 25 November 2020 . Accepted: 28 January 2021 . Published Online: 11 February 2021

Zahra Sabzevari, Reza Sahraei, Nawzad Nadhim Jawhar, Ahmet Faruk Yazici, Evren Mutlugun, and Ehsan Soheyli

Journal of Applied Physics ARTICLE scitation.org/journal/jap

Long-time stable colloidal Zn–Ag–In–S quantum dots with tunable midgap-involved emission

Cite as: J. Appl. Phys. **129**, 063107 (2021); doi: 10.1063/5.0038696
Submitted: 25 November 2020 · Accepted: 28 January 2021 ·
Published Online: 11 February 2021

View Online Export Citation CrossMark

Zahra Sabzevari,[1] Reza Sahraei,[1,a)] Nawzad Nadhim Jawhar,[2] Ahmet Faruk Yazici,[3] Evren Mutlugun,[4,a)] and Ehsan Soheyli[5,a)]

AFFILIATIONS

[1]Department of Chemistry, Faculty of Science, Ilam University, 65315-516 Ilam, Iran
[2]Department of Chemistry, College of Education, University of Garmian, 46021 Kalar, Iraq
[3]Department of Material Science and Nanotechnology Engineering, Abdullah Gul University, Kayseri 38080, Turkey
[4]Department of Electrical-Electronics Engineering, Abdullah Gul University, Kayseri 38080, Turkey
[5]Department of Physics, Faculty of Science, Ilam University, 65315-516 Ilam, Iran

Note: This paper is part of the Special Topic on Emerging Materials and Devices for Efficient Light Generation.

[a)]**Authors to whom correspondence should be addressed:** r.sahraei@ilam.ac.ir; evren.mutlugun@agu.edu.tr; and ehs.soheyli@gmail.com

ABSTRACT

Quaternary Zn–Ag–In–S (ZAIS) quantum dots (QDs) with efficient, tunable, and stable photoluminescence (PL) emission were prepared via a simple, effective, and low-cost reflux method. The structural analysis revealed the dominance of the quantum confinement effect. The calculated PL emission quantum yield was enhanced from 8.2% to 28.7% with experimental parameters indicating their marked influence on the PL emission properties of the final product. Particularly, it was found that by varying the precursors' feeding ratio, tunable emission from green to red was achieved. A set of direct and indirect pieces of evidence such as the broad-band emission spectrum (FWHM > 100 nm), large Stokes shift more than 120 nm, and predominantly a biexponentially long-lived decay profile with an average lifetime of about 366 ns were observed, showing the contribution of midgap localized energy levels in the recombination process. These data were obtained independently on the experimental condition used, which confirmed that this is mostly an intrinsic electronic property of quaternary In-based QDs. Finally, to ensure the stability of QDs in terms of colloidal and optical emission, their emission ability was evaluated after 26 months of storage. Colloidal QDs were still luminescent with strong yellowish-orange color with emission efficiency of ~20.3% after 26 months. The combination of synthesis simplicity, compositional non-toxicity, PL emission superiority (strong, tunable, stable, and long lifetime emission), and colloidal stabilities confirms that the present ZAIS QDs are promising candidates for a wide range of applications in biomedicine, anticounterfeiting, and optoelectronics.

I. INTRODUCTION

As more and more applications of semiconductor quantum dots (QDs) are existing in biotechnology and optoelectronic devices, the demand for the preparation of low-cost, non-toxic, and high-quality QDs has been on rise.[1–3] Among all types of structures, In-based QDs have received the utmost attention because they are emerging alternatives to the traditional toxic metal ion-based QDs.[4] These nanocrystals can be directly synthesized through a non-toxic, aqueous-based simple, efficient, and cost-effective colloidal process.[5] The dramatic increase in research activities on I-III-VI-based QDs is a direct consequence of their unique structural and optical advantages.[6] Particularly, structural disorders of I-III-VI QDs offer new opportunities due to their positive impact on their light emission characteristics.[7] Such Cd-free multinary compositions exhibited an unstructured absorption with determinative Urbach tail.[8] Raevskaya *et al.* demonstrated that Urbach energy and photoluminescence (PL) width increase considerably with a decrease in size of Ag–In–S QDs and assigned it to the contribution of defect-driven midgap levels into the recombination process.[9] These multinary semiconductor nanocrystals also

present a tunable emission across the visible spectrum that can extend to the near-infrared (NIR) region.[10,11] Besides, these structures are suitable for photovoltaic applications by possessing a variety of bulk band energies to cover the solar spectrum with high absorption coefficients.[12]

Efforts have been carried out to prepare aqueous-based colloidal Zn–Ag–In–S (ZAIS) QDs through various methods such as hydrothermal-assisted,[13] electrochemical,[14] and conventional reflux[15] approaches. While these are the most common methods used for the direct preparation of QDs and their derivatives in aqueous media, the reflux procedure outperforms by offering precise control and scalability of the synthesis. Besides, from the electronic-structure point of view, it has been approved that the defect-driven energy levels contribute remarkably to the PL emission of ZAIS QDs resulting in a broad inhomogeneous emission. Martynenko *et al.* evaluated the excitation energy dependence of different PL features of AIS/ZnS QDs supported by numerical modeling and revealed that there is a pronounced contribution of defect-related energy states at different energy positions.[8] Direct applications in white light-emitting diode,[14] photocatalysis,[16] bioanalysis,[17] anti-counterfeiting technology,[18] heavy-metal ion sensing,[19] and cellular imaging[20] are some of the promising uses of hydrophilic ZAIS QDs. Therefore, the preparation of luminescent ZAIS QDs possessing colloidal stability, emission tunability, and the long-lifetime feature is of great importance due to high demand in solar cells, [white] light-emitting diodes, and particularly for cellular bioimaging in nanomedicine. Recently, Schneider's group suggests a facile way to prepare 3-mercaptopropionic acid-capped AIZS QDs.[21] They evaluated the reaction parameters and showed that upon the size and composition-selective precipitations, the PL quantum yield (PLQY) can be enhanced to 78%, which is a quite high-level emission record for such aqueous-soluble structures. On the other hand, previous studies on the synthesis and optical properties of such QDs revealed that the optimization of experimental variables is a key factor for achieving high-quality materials.[20]

While the synthesis of luminescent colloids of I-III-VI-based QDs is a common work, they have a high-level tendency to crystallize in a multiphase structure with the non-luminescent feature. This is due to the simultaneous presence of various cations with quite different solubility products, which can be further observed in the direct-preparation of such multinary structures in a polar aqueous solvent. In this presented work, a colloidal reflux method has been employed to prepare luminescent ZAIS QDs with an intense and tunable emission character. The effect of different experimental parameters on the optical properties of as-prepared QDs was investigated to reach samples with reproducible optical character and PL QY of ~28.7% after a relatively short time of reaction. The energy levels that contributed to the recombination process were found to be the localized midgap levels with long lifetime character in the order of a few hundred nanoseconds. The as-prepared core-only colloidal QDs were highly stable with preserved emission property after a long time of more than 2 years. Strong emission remained noticeable after this time with PL QY of ~20.3%, nominating these stable QDs for various applications in biotechnology, optoelectronics, and anticounterfeiting.

II. EXPERIMENTAL SECTION

A. Materials

$ZnSO_4$ (Merck, ≥99%), $AgNO_3$ (Merck, 99.9%), $In(NO_3)_3$ (Merck, 99.99%), $C_5H_9NO_3S$ (NAC-Merck, ≥99%), $Na_3C_6H_5O_7$ (trisodium citrate dehydrate—TSC, Merck, 99%–101%), $Na_2S{\cdot}xH_2O$ (across organics, 60%–63%), NaOH (Merck, ≥99%), and CH_3COCH_3 (acetone, Merck, ≥99.8%) were used as received. De-ionized water was also used for all experiments.

B. Methods

A 70 ml aqueous solution containing 0.08 g NAC + 0.8 ml TSC (1M) + 125 μl $In(NO_3)_3$ (1M) + 0.6 ml $AgNO_3$ (0.02M) + 0.5 ml $ZnSO_4$ (0.1M) was titrated by NaOH (1M) at solution pH of 7. Then, it was transferred to the two-necked flask with a condenser attached and deaerated via nitrogen gas. After stirring for a while, 2 ml Na_2S (0.1M) was quickly injected into the stirring solution followed by an increase in reaction temperature to the desired value (60, 80, and 100 °C). Through the various reaction durations (15–360 min) at a specific temperature, heating and stirring were stopped to terminate the reaction and let it cool down to room temperature. The initial precursors' feeding ratio of In:NAC:TSC:Ag:Zn:Na_2S was 1:4:6.4:0.1:0.4:1.6. Optical measurements were performed at this step. To obtain fine powders for structural analysis, a specific amount of acetone was slowly added to the as-prepared colloidal QDs. When the solution turned opaque, a few drops of saturated NaOH solution added while stirring vigorously. Then, it was centrifuged and washed several times. The final products were dried overnight at room temperature.

C. Instruments

The absorbance characteristics of the as-prepared QDs were measured by a Cary 300 Bio UV-Vis spectrophotometer (VARIAN) at the wavelength range of 200–800 nm. The PL emission spectra of as-prepared QDs were recorded using a Cary Eclipse fluorescence spectrophotometer (Agilent technology). The crystallinity of synthesized particles was characterized using a Philips X'pert diffractometer in the 2θ range from 10° to 70°. The size and shape of the particles were observed under a FEI Talos F200S transmission electron microscope (TEM) at an operating voltage of 150 kV. The chemical composition and energy dispersive x-ray analysis (EDX)-mapping of samples were obtained by an energy dispersive x-ray analysis (EDX) instrument (Oxford INCA II energy solid-state detector). The time-resolved PL (TRPL) measurements were performed by PicoQuant Fluo Time 200 time-correlated single-photon counting (TCSPC) system equipped with a laser excitation source operating at 375 nm having a 500 kHz repetition rate. Lifetimes of the samples were collected with Time Harp 260 PICO system. The decay curves were modeled and amplitude average lifetimes were calculated by fitting the data with two exponentials using FluoFit software by PicoQuant Technologies.

III. RESULTS AND DISCUSSION

A. EDX/EDX-mapping

To ensure the key contribution of all chemical elements, the EDX analysis was performed (Fig. 1). As expected then, the

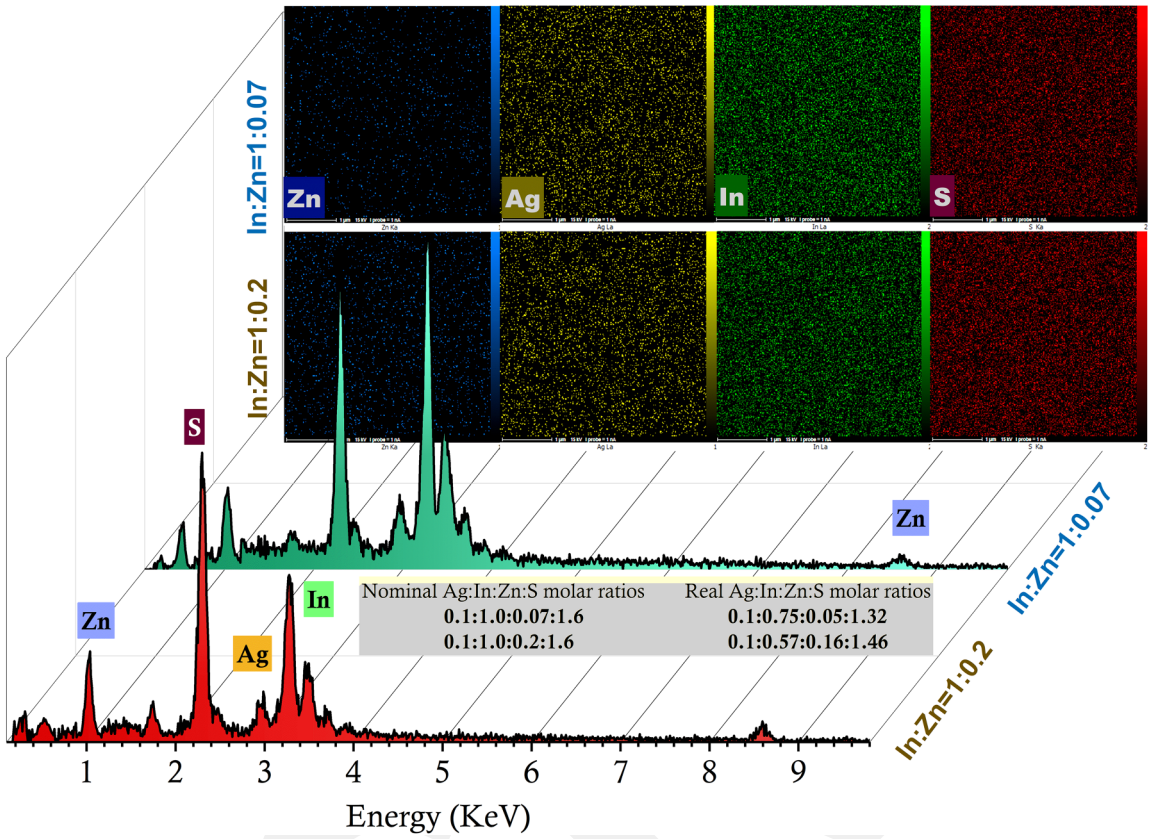

FIG. 1. EDX and EDX-mapping results for ZAIS QDs prepared at two different In:Zn molar ratios (at solution pH of 7.6, the refluxing temperature of 100 °C, and reaction time of 120 min). Inset shows the nominal and real molar ratios of constituent elements.

characteristic peaks of Zn, Ag, In, and S were recorded in the EDX profile, supported by qualitative data of EDX-mapping. Based on EDX measurements, the feeding molar ratios of Ag:In:Zn:S used in the reaction solution and the real Ag:In:Zn:S molar ratios in the QDs composition were determined and are given at the inset of Fig. 1. It can be seen that with an increase in Zn content in the reaction solution, the Zn amount in ZAIS QDs also increases. Since the solubility product of In–S is smaller than Ag–S and Zn–S bonds, QDs are In-rich compositions (as recorded data indicate). Such condition facilitates the formation of substitutional indium and silver vacancy sites, which is suitable for radiative emissions.[22]

B. XRD and TEM

ZAIS-derivative QDs have been crystallized in different crystalline phases. Some researchers reported cubic and orthorhombic (JCPDS 00-025-1329/00-025-1328) phase structures for homogenous alloy ZAIS QDs,[10,13] while others reported tetragonal chalcopyrite (JCPDS 00-025-1330/01-075-0117)[21,23] and hexagonal (JCPDS 01-089-502) crystal phases, respectively.[24] The XRD pattern of ZAIS QDs prepared at this work with two In:Zn molar ratios along with standard patterns of several multinary bulk structures are shown in Fig. 2(a). The patterns show a quite broad peak located about 27° along with quite broader peaks at 47° and 53°. The weakness and broadness of diffraction peaks as well as the high-density of intrinsic lattice defects in such multinary structures making it a bit difficult to precisely identify the type of crystalline phases. On the other hand, the XRD peak experiences a very slight shift toward higher scattering angles upon an increase in Zn concentration, which can be ascribed to a smaller ionic radius of Zn^{2+} ions (0.74 Å) rather than other presented cations.

All the fundamental and technological merits of semiconductor nanocrystals are due to their size and shape-driven properties, particularly, at the size-regime below their excitonic Bohr radius. TEM images give us direct conclusions about the size and shape of the nanocrystals [Fig. 2(b)]. Nearly all of the reports in the literature on the aqueous media synthesis approach were based on quasi-spherical shape. Because the thiol (–SH) group of NAC has a very strong affinity for QDs due to a soft–soft interaction.[25] As can be seen in Fig. 2(b), the prepared semiconductor nanocrystals have a non-uniform quasi-spherical shape with an average size of about 6.8 nm and a relatively broad size distribution. The result indicates that samples are three-dimensionally confined

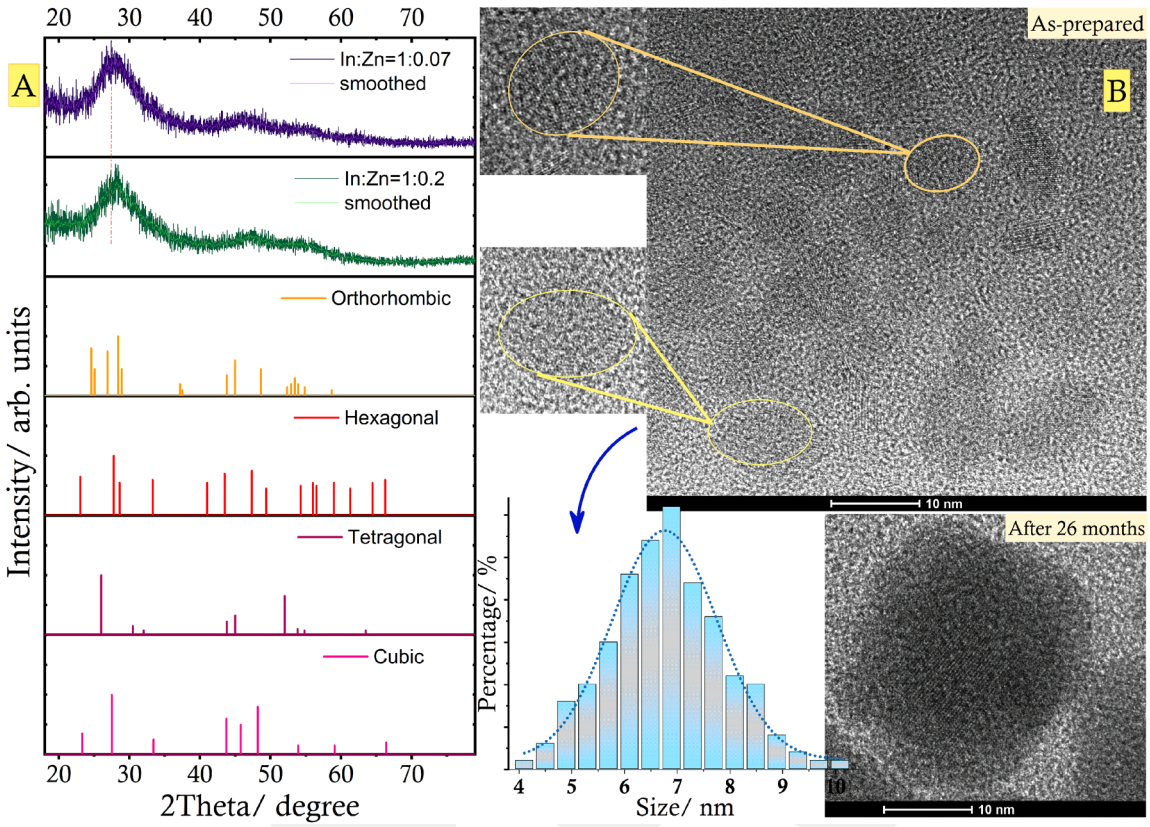

FIG. 2. (a) XRD patterns (prepared at two different In:Zn molar ratios) along with standard lines for XRD patterns of various (Ag–In–S)-based bulk structures and (b) typical TEM image and size distribution profile of ZAIS QDs prepared at solution pH of 7.6, refluxing temperature of 100 °C, and reaction time of about 120 min. The TEM image of the same QDs after 26 months of storage has been also included.

structures within the strong confinement regime. The lattice fringes are somehow observable in the inset of Fig. 2(b) implying the crystalline nature of the QDs after 26 months of preparation. This image demonstrates the great structural and colloidal stability of QDs after long-time storage. On the other hand, it shows a remarkable increase in the size of QDs after long-time storage that can be assigned to the growth of QDs and leads to a red-shift in the PL emission spectrum. Finally, the interplanar distance has been measured as 0.369 nm. This value reveals the formation of an orthorhombic structure with alloyed Zn–Ag–In–S character because, in the case of a tetragonal phase structure, the interplanar distance should be much smaller.[26]

IV. OPTICAL OPTIMIZATIONS

The TRPL measurement was carried out for typical ZAIS QDs prepared at a reaction temperature of 100 °C (Fig. 3). The decay profile fitted by a bi-exponential function showed distinct slow and fast decay components of $A_1 = 572.81 \pm 9.08/\tau_1 = 478.8 \pm 7.0$ ns and $A_2 = 236.6 \pm 27.4/\tau_2 = 95.3 \pm 13.5$ ns, respectively. τ represents the exciton lifetime through different recombination pathways and A stands for the coefficient of corresponding decay lifetime. Both data showed a long-lifetime characteristic that is within the range expected for the midgap-levels' decay lifetime. Nonetheless, the contributed energy levels must be different due to the noticeable difference between decay rates of τ_1 and τ_2. The shorter lifetime can be assigned to recombinations through surface trap sites (shallow trap levels), whereas the longer one can be assigned intrinsic trap state (deep donor–acceptor)-involved recombinations.[13] Dangling bonds (unpassivated species) are the most known origins for capturing the photoexcited charge carriers as surface trap states. These sites usually arise due to the shallow energy states within the bandgap region with relatively fast-decay character. On the other hand, vacancies and interstitial atoms are considered intrinsic defects that are responsible for deep trap states. The dominance of the slower component is also obvious in the present work. This indicates that while the surface trap sites still get involved in recombination processes, the recombination processes are mainly performed via intrinsic donor–acceptor states. The average amplitude decay lifetime $\left(\tau_{avg} = \sum_i A_i\tau_i / \sum_i A_i\right)$ is therefore

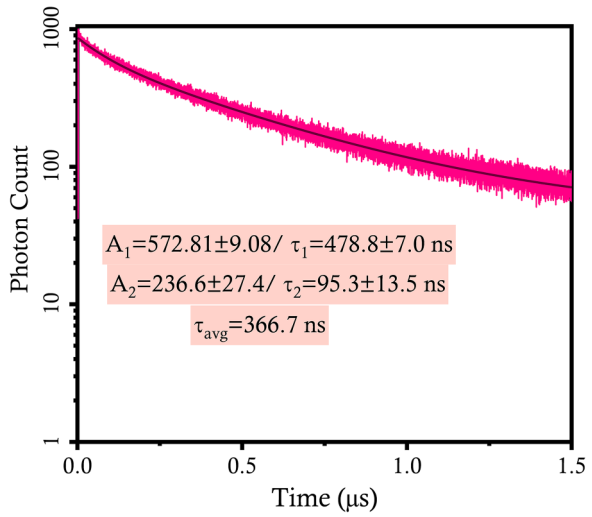

FIG. 3. TRPL profile of typical ZAIS QDs prepared at the refluxing temperature of 100 °C, solution pH = 7.6, and the In:NAC:TSC:Ag:Zn:Na_2S feeding ratio of 1:4:6.4:0.1:0.4:1.6.

around average PL lifetime (τ_{avg}) = 366.7 ns, which is a quite long record for inorganic fluorescent QDs. The recorded value is at the range of average PL lifetime of Zn–$AgIn_5S_8$ QDs prepared by Zhang *et al.* and those reported for ZAIS QDs prepared by Chen *et al.*[16,27] These data confirm that the excitonic states are not included in the recombination process, and the midgap defect levels are responsible for recombination properties of present colloidal ZAIS QDs. It has been reported that donor–acceptor radiative recombinations are carried out mainly through silver vacancies and indium substitutions presented in AIS–ZnS QDs.[22]

A. Effect of reaction temperature

Figure 4(a) shows the UV-Vis and PL spectra of as-prepared ZAIS QDs at different reaction temperatures (at solution pH = 7 and feeding ratio of In:NAC:TSC:Ag:Zn:Na_2S = 1:4:6.4:0.1:0.4:1.6). As can be seen, as the reaction temperature increases, a gradual increase in the absorption intensity of the UV-Vis spectra is observed in the absorption edge region. This excitonic-excluded absorption edge (the absence of sharp absorption peak) is a characteristic feature of such nanostructures, which shows a slight red-shift with reaction temperature from 440 to 475 nm. It can be attributed to the faster growth of QDs at high reaction temperature (100 °C), which results in the formation of larger QDs. In order to assess the emission properties of as-synthesized QDs, they were excited by an excitation wavelength of 380 nm. A broad and intense peak located near 560 nm was obtained. Recorded data revealed that PL emission intensity was enhanced with an increase in the reaction temperature. This can be attributed to the increase in the size of QDs and thus the decrease in their surface to volume ratio, which can reduce the non-radiative surface-related energy levels.[28] High reaction temperature also improves the crystallinity of prepared QDs via reduction of structural and surface defects. The PL QYs of as-prepared ZAIS QDs at different experimental parameters were calculated by the method as reported elsewhere via fluorescein as a reference dye.[29] The calculated PL QYs at reaction temperatures of 60, 80, and 100 °C were 8.7%, 10.2%, and 13.2%, respectively. Therefore, the temperature of 100 °C was considered for further experiments. More importantly, the large Stokes shift of around 85–120 nm, FWHM of about 130–140 nm, and approximately temperature-independent property of emission wavelength indicate that the midgap states are responsible for the recombination of charge carriers.[30] These data are in excellent correspondence with the TRPL data recorded for the colloidal sample. The absence of absorption peak onset and PL FWHM > 100 nm are typical pieces of evidence for a quaternary compound.[31]

B. Effect of solution pH

A remarkable effect of solution pH on the absorption and PL emission spectra of as-prepared ZAIS QDs are shown in Fig. 4(b). An increase in solution pH to change the neutralized medium toward a slightly basic solution leads to a nonlinear variation in both absorption and PL spectra. The best PL QY was calculated for pH = 7.6 at about 22.7%, whereas it demonstrated a remarkable decrease upon increasing the pH to 8.5. Besides, at the solution pH of 8.5, a clear red-shift along with an increase in the absorbance is observed in the longer wavelengths region, which could be the result of the aggregation of QDs at high pH values. While NAC molecules can be deprotonated easily at basic medium to provide better surface passivation (via two functional groups of thiol and amino), different cations used in such structures have very different chemical natures. Indeed, In^{3+} ions (hard acid) are much more reactive toward S^{2-} ions (soft base) than Zn^{2+} (soft acid) and Ag^{+} (soft acid) ions. Therefore, a mild acid–base reaction media should be used to prepare multinary stable QDs without considerable phase separation or formation of cationic hydroxide precipitates.[32] High pH value can also facilitate the corporation of excess S^{2-} ions into the reaction media, leading to QDs with a high density of defects or unpassivated surface states. Such observations have been reported elsewhere.[33,34]

C. Effect of precursors solution concentration

To examine the effects of precursor's concentration, the concentration of precursors solution was changed. Different concentrations were calculated by considering the amount of all cations used in the reaction solution ([In + Ag + Zn]), while the feeding ratio of In:NAC:TSC:Ag:Zn:Na_2S (1:4:6.4:0.1:0.4:1.6) remained constant. As can be seen in Fig. 4(c), with an increase in the concentration of precursors the absorption edge goes toward a longer wavelength, and absorption intensity is enhanced. Both these outcomes showed an increase in the concentration of prepared QDs in aqueous colloids. On the other hand, with an increase in precursor concentrations, the best PL QY of about 22.7% was obtained at a precursors solution concentration of 2.7 mM, while there is no significant change in emission wavelength.

D. In:NAC molar ratio

Various sorts of molecules can be used for electrostatic or steric control of the growth of the QDs in the colloidal medium.

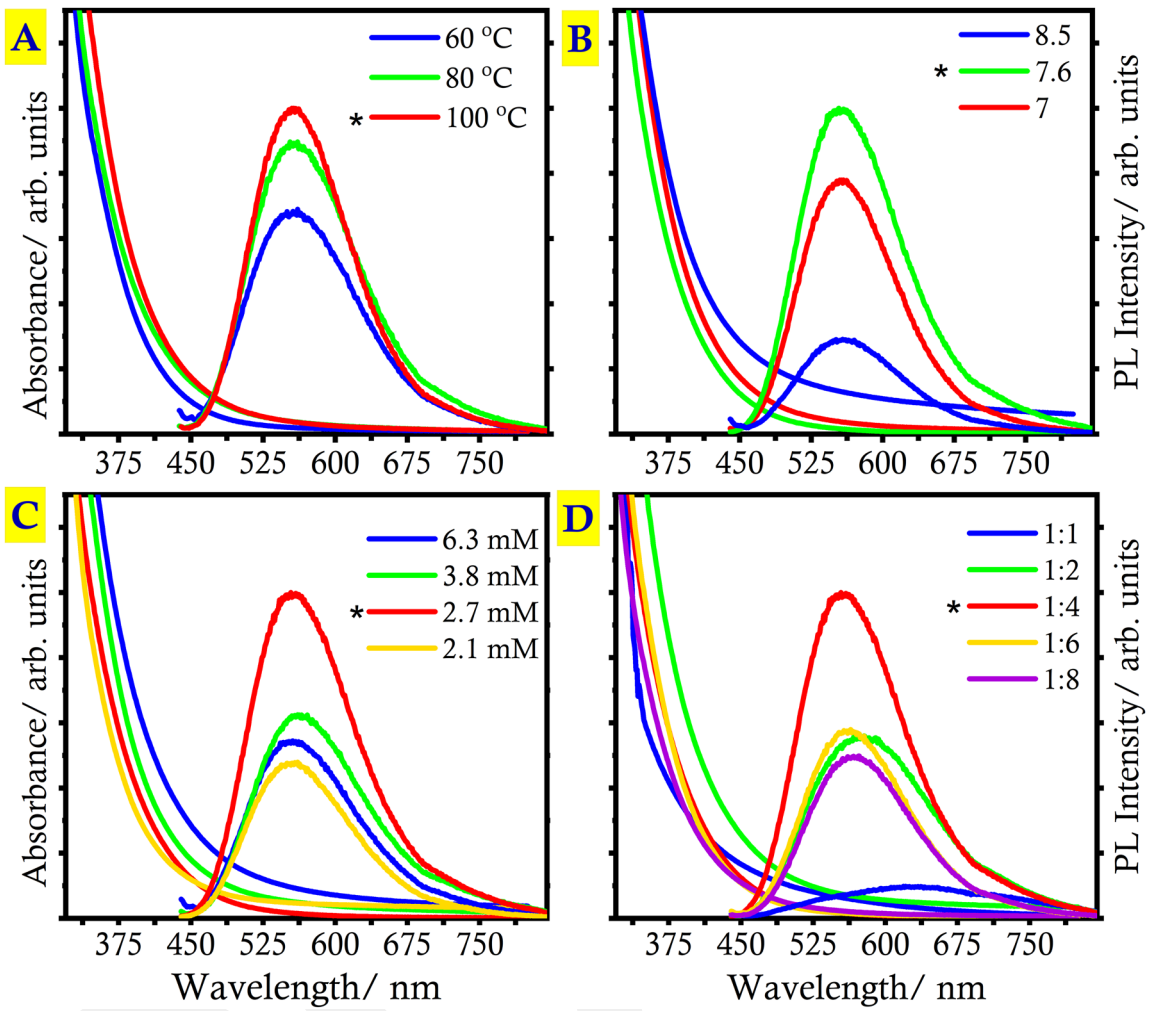

FIG. 4. The UV-Vis absorption and PL emission spectra (λ_{exc} = 420 nm) of ZAIS QDs prepared at different (a) reaction temperatures, (b) solution pH, (c) precursors' solution concentration, and (d) feeding ratio of In:NAC. Star signs show the best emission results.

They can also play the role of surface capping agent, improving the emission brightness and stability of the colloid. In this presented work, NAC thiol molecules were used for this purpose, in such a way that at the lowest amount of NAC (0.02 g, In:NAC = 1:1) the PL emission intensity is quite low with a long tale absorption [Fig. 4(d)]. The obvious red-shift (compared to other In:NAC ratios) in both spectra for In:NAC = 1:1 can be attributed to the faster growth rate of QDs in the absence of a sufficient amount of NAC capping agent. It is worth noting that the colloid of as-prepared ZAIS QDs was opaque at this condition demonstrating the stabilizing role of NAC. Nonetheless, a significant enhancement in PL emission intensity was investigated, following an increase in the amount of NAC precursor (to 0.08 g, In:NAC = 1:4). The best PL QY of around 22.7% was recorded at In:NAC molar ratio of 1:4. This confirms that the NAC ligands have an effective role in the passivation of surface dangling bonds.[34] It can be observed that the overall effect of an increase in the amount of NAC is blue-shift in optical spectra (from 550 to 460 nm), which can be ascribed to the slower growth-rate of QDs due to prominent steric/electrostatic repulsion of NAC capping molecules. On the other hand, the excess amount of NAC ligand leads to a reduction in PL emission intensity probably due to the formation of new non-radiative recombination centers at the surface of QDs.[13]

E. In:TSC molar ratio

Due to the multi-cationic character of such structures with soft and hard base natures, the presence of a second hard base stabilizer is required. Similar to the concentration effect of NAC, there is a remarkable blue-shift in both spectra with an increase

in the amount of TSC [Fig. 5(a)]. The PL emission profile shifts from red emission at ~630 nm (In:TSC = 1:3.2) to green emission at ~554 nm (In:TSC = 1:6.4). This observation demonstrates the versatility of the suggested simple route to reach an intense and tunable PL emission in the wide color range of the visible spectrum. The PL emission intensity became stronger and reached a maximum at In:TSC = 1:6.4 (with PL QY of around 22.7%), whereas a further increase in the amount of TSC would cause a decrease in PL intensity.

F. In:Ag molar ratio

One of the key parameters in multi-element compounds is the relative amount of the main cations and anions. The absorption and PL emission spectra of ZAIS QDs [Fig. 5(b)] show that the decrease in the Ag amount used in the synthesis of QDs results in a clear blue-shift in absorption edge wavelength and a slight one in the PL emission peak. These can be attributed to a difference in the bandgap energy of bulk In_2S_3 (2.3 eV) and Ag_2S (1.0 eV) lattice structures.[35] The valence-band edge in ZAIS QDs consists of the hybridization of Ag_{3d} and S_{3p} orbitals, including a repulsive force between these orbitals.[27] Upon a decrease in Ag concentration (increase in In:Ag molar ratio), repulsive force reduces, which results in a gradual increase in bandgap energy and successive blue-shift in optical spectra. The decrease in Ag concentration (up to a certain amount) further facilitates the presence of the proper density of silver vacancy and substitutional indium sites, which leads to an increase in donor–acceptor radiative recombinations and

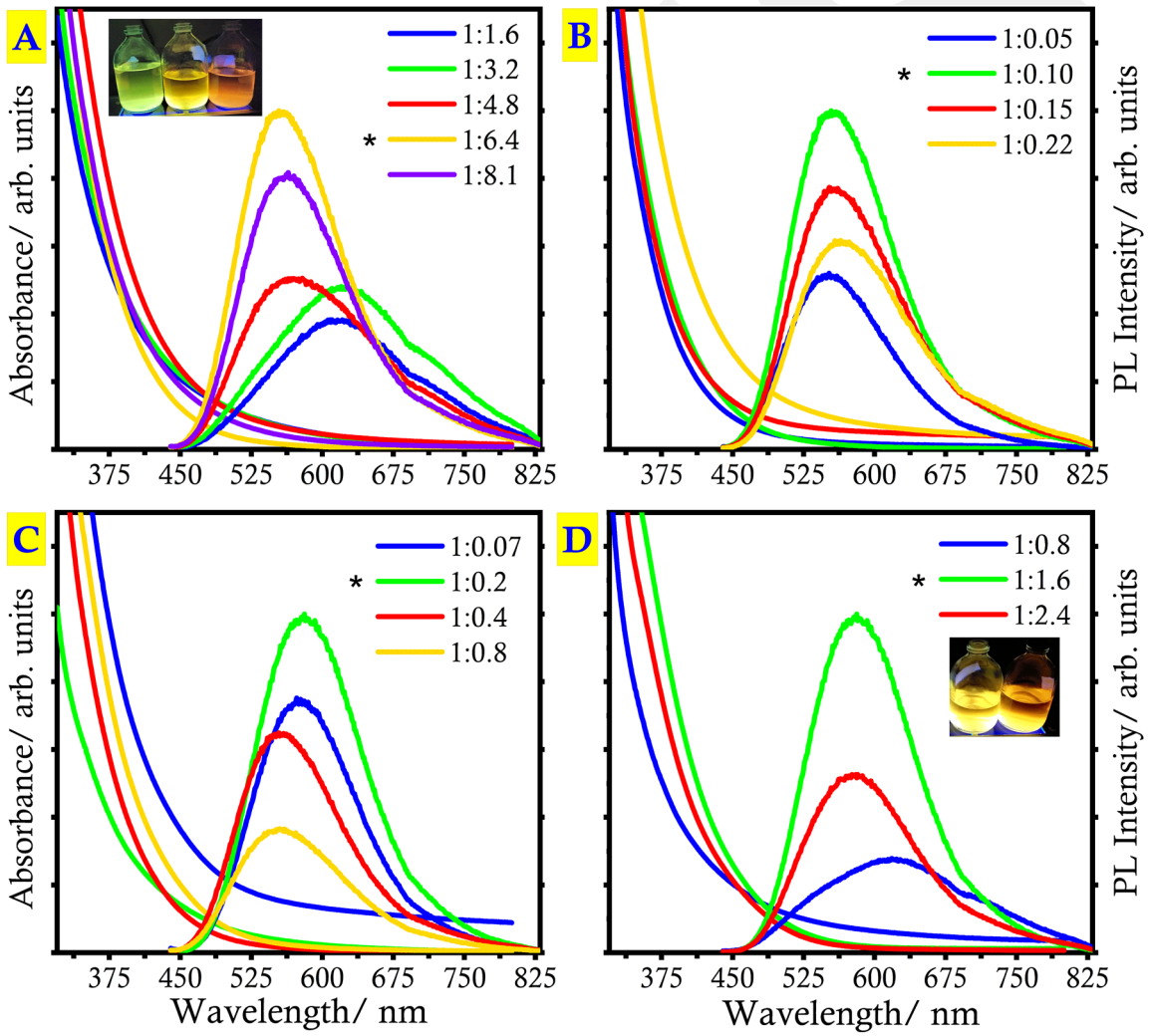

FIG. 5. The UV-Vis absorption and PL emission spectra (λ_{exc} = 420 nm) of ZAIS QDs prepared at different feeding ratio of precursors; (a) In:TSC (Inset: A digital image of colloidal QDs under 365 nm/6 W irradiation), (b) In:Ag, (c) In:Zn, and (d) In:Na_2S (inset: A digital image of colloidal QDs under 365 nm/6 W irradiation). (Reaction performed at a solution pH of 7.6, the refluxing temperature of 100 °C, and a reaction time of about 120 min). Star signs show the best emission results.

an ensuing increase in emission intensity. The PL emission intensity reached the maximum at an In:Ag feeding ratio of 1:0.10 (with PL QY of around 22.7%), followed by a tail-off with further increasing the Ag amount.

G. In:Zn molar ratio

Figure 5(c) shows the optical properties of as-synthesized ZAIS QDs at different feeding ratios of In:Zn. At the low concentration of the zinc precursor, the absorption edge and PL emission peak are located near 486 nm and 573 nm, respectively. As seen in Fig. 5(c), as the amount of zinc precursor increased (up to In:Zn molar ratio of 1:0.8), a blue-shift has been recorded for both spectra, which is due to the increase in the bandgap energy of QD composition at a higher level of Zn precursor ($E_g^{ZnS} = 3.6$ eV > $E_g^{AgInS} = 1.87$–2.03 eV). Such composition-dependent tunability in optical properties with a longer-lived emission character has been reported elsewhere for aqueous-soluble ZAIS QDs.[18] The optimal PL emission efficiency was obtained at In:Zn molar ratio of 1:0.2 (which has been attributed to the initial quench in nonradiative surface sites and enhancement of radiative intrinsic states). The best PL QY was near 28.7%. However, excess amounts of Zn precursor make the radiative recombination centers close to each other, which dominates undesired interaction among charge carriers and nonradiative recombinations.[36]

H. In:Na_2S molar ratio

The presence of sufficient anion sites to create a well-structured cation–anion lattice is a vital factor governing the physicochemical properties of the nanocrystalline materials. Among the probable candidates to play the role of anion precursor in multinary QDs, sodium sulfide has the highest reactivity.[20] As can be seen in Fig. 5(d), a remarkable blue-shift is detectable for both absorption and emission results, owing to a change in emission color from red to yellow. The PL emission intensity was initially enhanced, followed by a significant reduction in higher amounts of Na_2S. When the amount of Na_2S is too high, the surface of bare ZAIS QDs would have an anionic-rich character that reduces the formation possibility of cation-thiol complex shell on the QDs' surface. This decreases the surface passivation strength of the NAC and TSC ligands and quenches the emission intensity.[37] The best emission efficiency of near 28.7% has been obtained at an In:Na_2S molar ratio of 1:1.6.

I. Reaction time

Optimization of the reaction time is essential and depends on the experimental procedure, the reaction medium, and the parameters used. In general, prolonging the refluxing time in the aqueous-based synthesis of QDs leads to a red-shift in the absorption edge of samples, which is due to the growth of QDs and thus the reduction of their bandgap energy accordingly. These would lead to a mutual change in both absorption and emission spectra of the present multinary In-based QDs. As Fig. 6 shows, while a wavelength red-shift in the absorption edge is quite obvious, there is only a slight red-shift in the emission peak demonstrating that the change in reflux time is not a favorable way to tune the emission

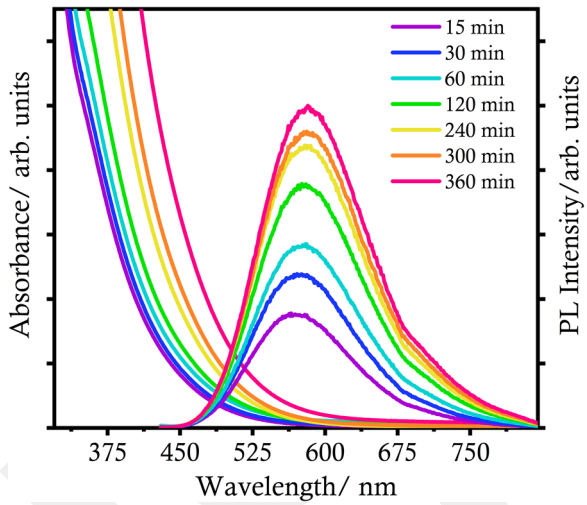

FIG. 6. The UV-Vis absorption and PL emission spectra ($\lambda_{exc} = 420$ nm) of ZAIS QDs prepared at different refluxing times (reaction performed at a solution pH of 7.6, the refluxing temperature of 100 °C, and In:NAC:TSC:Ag:Zn:Na_2S molar ratios of 1:4:6.4:0.1:0.2:1.6).

color in such a midgap-dominant ZAIS QDs. The PL emission wavelength shifted from 572 to 582 nm upon an increase in reaction time from 15 to 360 min. As the deep/shallow trap states are mainly involved in the recombination process of such structures, they can be influenced less/more by quantum confinement effects and experience a smaller shift in their energies. Upon an increase in reaction time, the PL QYs at different refluxing times of 15, 30, 60, 120, 240, 300, and 360 are 15.8, 18.4, 22.1, 28.7, 21.3, 19.2, and 14.1, respectively. Therefore, the best emission efficiency was obtained at a refluxing time of 120 min with a PL spectrum located around 576 nm.

J. Stability of as-prepared ZAIS QDs

Both the colloidal and optical stabilities of colloidal QDs are always of great importance as an indicative factor for any application in biotechnology and optoelectronic devices. To confirm the colloidal superiority of the aqueous-soluble QDs in this work, colloidal QD with optimized emission was kept at the refrigerator for a long time (~26 months), and the PL emission characteristics were reassessed (Fig. 7). The obtained data revealed that the samples preserve the photoluminescent properties along with a bright yellow-orange emission after a long time. In comparison with the PL data reported for as-prepared QDs after refluxing time of 120 min, 22 nm red-shift was recorded which can be attributed to the growth or just partial aggregations of QDs. This is in complete accordance with TEM results in Fig. 2(b) which showed an increase in the size of QDs after 26 months of storage. The calculated PL QY was 20.3%, which is a high record for aqueous-based ZAIS QDs after long-time storage. The contour-plot of PL excitation spectra has been shown, further supporting the results. It should be noted that the samples with an

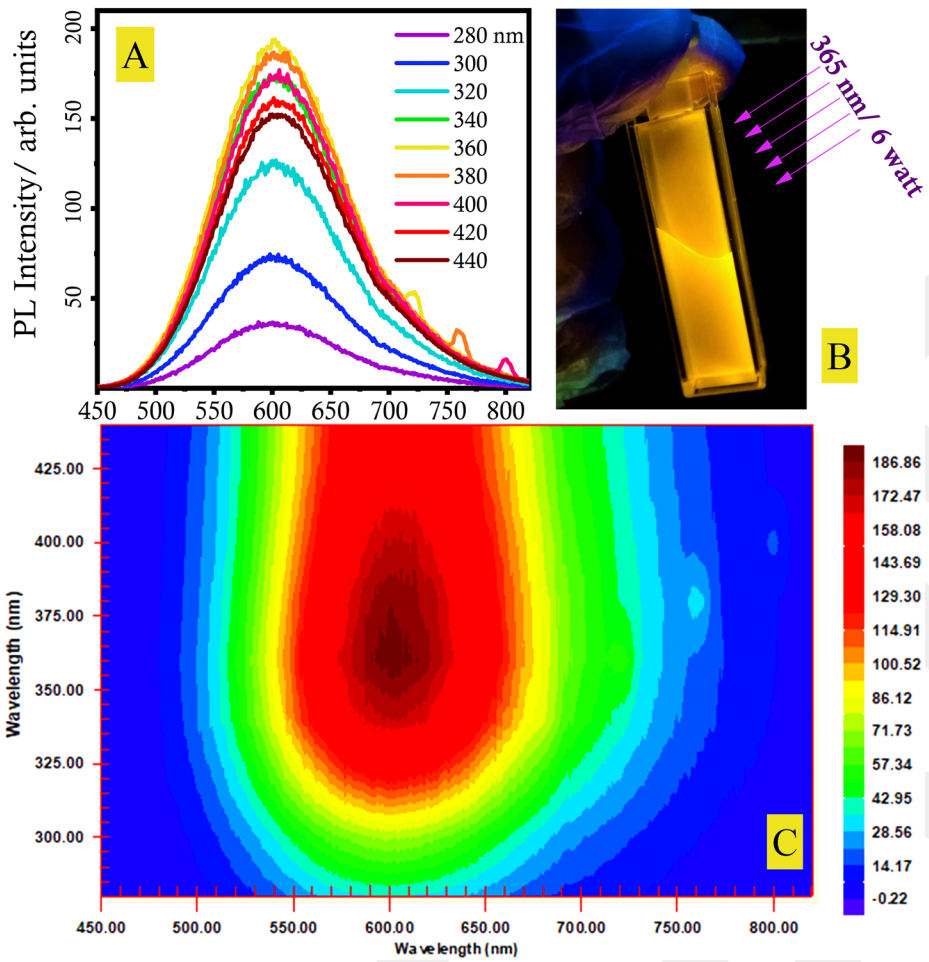

FIG. 7. (a) The PL emission spectra at different excitation wavelengths, (b) corresponding digital image of colloidal ZAIS QDs under 365 nm/6 W irradiation after 26 months of initial preparation, and (c) contour-color fill profile (at different excitation wavelengths). The vertical axis of the contour plot is the excitation wavelength.

insufficiently low amount of ligands, excess amounts of precursors, or high pH were not as stable as other samples.

V. CONCLUSIONS

The hydrophilic ZAIS colloidal QDs have been prepared using *N*-acetyl-L-cysteine and trisodium citrate as capping agents, employing a colloidal reflux method. The as-synthesized ZAIS QDs were found to have spherical-shape with sub-10 nm size. The energy-dispersive x-ray (EDX) and EDX-mapping experiments demonstrated the presence of all expected elements with an In-rich characteristic. Considering the importance of the optical properties of QDs, the most attention was paid to the optimization of their photoluminescence (PL) property. Various experimental parameters such as reaction temperature, solution pH, the concentration of QDs, the molar ratio of precursors, and reaction time were optimized, and the evaluation of UV-Vis and PL spectra was recorded. It was found that all samples have a broad absorption region attributed to the intrinsic defect sites within such In-chalcogenide nanostructures. On the other hand, a relatively broad and intense emission peak with a large Stokes shift was observed in each case. These results support the effective role of defect energy levels (localized inside the bandgap energy) in the excitation and recombination of charge carriers. More importantly, by varying the precursors' molar ratio, a tunable/intense emission was obtained, which further demonstrates the success of our method to reach high-quality QDs with applicable emission characteristics. The simplicity and cost-effectiveness of the present direct aqueous-based preparation method, along with the formation of high-quality QDs with tunable/intense (PL QY of about 28.7% and 20.3% after 26 months)/long-term emission, and excellent colloidal stability are notable results, nominating the present ZAIS QDs for future applications in nanomedicine, sensing, and optoelectronics.

AUTHORS' CONTRIBUTIONS

Z.S. contributed to investigation and formal analysis. R.S. contributed to project administration, conceptualization, funding acquisition, resources, validation, writing-review, and editing. N.N.J. contributed to investigation and formal analysis. A.F.Y. contributed to formal analysis, validation, and data curation. E.M. contributed to resources, validation, writing-review, and editing. E.S. contributed to

conceptualization, data curation, methodology, validation, visualization, writing-original draft, writing-review, and editing.

DATA AVAILABILITY

The data that support the findings of this study are available from the corresponding author upon reasonable request.

REFERENCES

[1]F. Huo, Y. Liu, M. Zhu, E. Gao, B. Zhao, and X. Yang, ACS Appl. Mater. Interfaces **11**, 27259–27268 (2019).
[2]B. Huang, Q. Dai, N. Zhuo, Q. Jiang, F. Shi, H. Wang, H. Zhang, C. Liao, Y. Cui, and J. Zhang, J. Appl. Phys. **116**, 094303 (2014).
[3]B. Liu, Y. Altintas, L. Wang, S. Shendre, M. Sharma, H. Sun, E. Mutlugun, and H. V. Demir, Adv. Mater. **32**, 1905824 (2020).
[4]A. C. Berends, M. J. J. Mangnus, C. Xia, F. T. Rabouw, and C. De Mello Donega, J. Phys. Chem. Lett. **10**, 1600 (2019).
[5]E. Soheyli, B. Ghaemi, R. Sahraei, Z. Sabzevari, S. Kharrazi, and A. Amani, Mater. Sci. Eng. C **111**, 110807 (2020).
[6]O. Yarema, M. Yarema, and V. Wood, Chem. Mater. **30**, 1446–1461 (2018).
[7]V. K. Komarala, C. Xie, Y. Wang, J. Xu, and M. Xiao, J. Appl. Phys. **111**, 124314 (2012).
[8]I. V. Martynenko, A. S. Baimuratov, F. Weigert, J. X. Soares, L. Dhamo, P. Nickl, I. Doerfel, J. Pauli, I. D. Rukhlenko, A. V. Baranov, and U. Resch-Genger, Nano Res. **12**, 1595 (2019).
[9]A. Raevskaya, V. Lesnyak, D. Haubold, V. Dzhagan, O. Stroyuk, N. Gaponik, D. R. T. Zahn, and A. Eychmüller, J. Phys. Chem. C **121**, 9032 (2017).
[10]J. Song, C. Ma, W. Zhang, X. Li, W. Zhang, R. Wu, X. Cheng, A. Ali, M. Yang, L. Zhu, R. Xia, and X. Xu, ACS Appl. Mater. Interfaces **8**, 24826 (2016).
[11]Y. Gao, H. Liu, J. Li, S. Xiao, Z. Guo, R. Pan, X. Lin, and T. He, J. Phys. D: Appl. Phys. **53**, 255103 (2020).
[12]A. Khorasani, M. Marandi, R. Khosroshahi, M. Malekshahi Byranvand, M. Dehghani, A. I. Zad, F. Tajabadi, and N. Taghavinia, ACS Appl. Mater. Interfaces **11**, 30838 (2019).
[13]J. Song, T. Jiang, T. Guo, L. Liu, H. Wang, T. Xia, W. Zhang, X. Ye, M. Yang, L. Zhu, R. Xia, and X. Xu, Inorg. Chem. **54**, 1627 (2015).
[14]F. L. N. Sousa, D. V. Freitas, R. R. Silva, S. E. Silva, A. C. Jesus, H. S. Mansur, W. M. Azevedo, and M. Navarro, Mater. Today Chem. **16**, 100238 (2020).
[15]Y. Liu, X. Tang, M. Deng, T. Zhu, Y. Bai, D. Qu, X. Huang, and F. Qiu, J. Lumin. **202**, 71 (2018).
[16]D. Zhang, W. Cao, B. Mao, Y. Liu, F. Li, W. Dong, T. Jiang, Y. C. Yong, and W. Shi, Ind. Eng. Chem. Res. **59**, 16249–16257 (2020).
[17]C. Q. Zhao, S. N. Ding, J. J. Xu, and H. Y. Chen, ACS Appl. Nano Mater. **3**, 11489 (2020).
[18]Y. Chen, Q. Hu, Q. Wang, M. Yu, X. Gong, S. Li, J. Xiao, Y. Guo, G. Chen, and X. Lai, RSC Adv. **10**, 23410 (2020).
[19]Y. Liu, X. Tang, M. Deng, T. Zhu, L. Edman, and J. Wang, "Hydrophilic AgInZnS quantum dots as a fluorescent turn-on probe for Cd^{2+} detection," J. Alloys Compd. (to be published); available at https://www.sciencedirect.com/science/article/pii/S0925838820344728.
[20]D. Deng, J. Cao, L. Qu, S. Achilefu, and Y. Gu, Phys. Chem. Chem. Phys. **15**, 5078 (2013).
[21]M. Mrad, T. Ben Chaabane, H. Rinnert, B. Lavinia, J. Jasniewski, G. Medjahdi, and R. Schneider, Inorg. Chem. **59**, 6220 (2020).
[22]T. Chevallier, A. Benayad, G. Le Blevennec, and F. Chandezon, Phys. Chem. Chem. Phys. **19**, 2359 (2017).
[23]Y. Huang, H. Lin, J. Qiu, Z. Luo, Z. Yao, L. Liu, H. Liu, X. Tang, and X. Fu, J. Mater. Chem. C **8**, 7734 (2020).
[24]T. Kameyama, S. Koyama, T. Yamamoto, S. Kuwabata, and T. Torimoto, J. Phys. Chem. C **122**, 13705 (2018).
[25]D. Bain, B. Paramanik, S. Sadhu, and A. Patra, Nanoscale **7**, 20697 (2015).
[26]P. Bujak, Z. Wróbel, M. Penkala, K. Kotwica, A. Kmita, M. Gajewska, A. Ostrowski, P. Kowalik, and A. Pron, Inorg. Chem. **58**, 1358 (2019).
[27]T. Chen, Y. Ren, Y. Xu, W. Jiang, L. Wang, W. Jiang, and Z. Xie, J. Alloys Compd. **858**, 158084 (2021).
[28]N. N. Jawhar, E. Soheyli, A. F. Yazici, E. Mutlugun, and R. Sahraei, J. Alloys Compd. **824**, 153906 (2020).
[29]E. Soheyli, R. Sahraei, and G. Nabiyouni, J. Lumin. **205**, 525 (2019).
[30]S. Gardelis, M. Fakis, N. Droseros, D. Georgiadou, A. Travlos, and A. G. Nassiopoulou, J. Phys. D: Appl. Phys. **50**, 035107 (2017).
[31]D. Deng, L. Qu, Z. Cheng, S. Achilefu, and Y. Gu, J. Lumin. **146**, 364 (2014).
[32]A. Arshad, H. Chen, X. Bai, S. Xu, and L. Wang, Chin. J. Chem. **34**, 576 (2016).
[33]N. Zikalala, S. Parani, N. Tsolekile, and O. S. Oluwafemi, J. Mater. Chem. C **8**, 9329 (2020).
[34]J. Song, C. Ma, W. Zhang, S. Yang, S. Wang, L. Lv, L. Zhu, R. Xia, and X. Xu, J. Mater. Chem. B **4**, 7909 (2016).
[35]P. Y. Lai, C. C. Huang, T. H. Chou, K. L. Ou, and J. Y. Chang, Acta Biomater. **50**, 522 (2017).
[36]D. K. Sharma, S. Hirata, L. Bujak, V. Biju, T. Kameyama, M. Kishi, T. Torimoto, and M. Vacha, Phys. Chem. Chem. Phys. **19**, 3963 (2017).
[37]E. Soheyli, D. Azad, R. Sahraei, A. A. Hatamnia, A. Rostamzad, and M. Alinazari, Colloids Surf. B **182**, 110389 (2019).